Proceedings of GT2005
ASME Turbo Expo 2005: Power for Land, Sea and Air
June 6-9, 2005, Reno-Tahoe, Nevada, USA

GT2005-68100

# EXPERIMENTAL RESULTS AND TRANSIENT MODEL VALIDATION OF AN EXTERNALLY FIRED MICRO GAS TURBINE

**Alberto Traverso**
TPG-DiMSET
Università di Genova, Genoa, Italy
alberto.traverso@unige.it

**Riccardo Scarpellini**
Ansaldo Ricerche s.r.l.
Genoa, Italy
scarpel@ari.ansaldo.it

**Aristide Massardo**
TPG-DiMSET
Università di Genova, Genoa, Italy
massardo@unige.it

## ABSTRACT

This paper presents the performance of the world's first Externally Fired micro Gas Turbine (EFmGT) demonstration plant based on micro gas turbine technology.

The plant was designed by Ansaldo Ricerche (ARI) s.r.l. and the Thermochemical Power Group (TPG) of the Università di Genova, using the in-house TPG codes TEMP (Thermoeconomic Modular Program) and TRANSEO. The plant was based on a recuperated 80 kW micro gas turbine (Elliott TA-80R), which was integrated with the externally fired cycle at the ARI laboratory. The first goal of the plant construction was the demonstration of the EFmGT system at full and part-load operations, mainly from the control point of view. The performance obtained in the field can be improved in the near future using high-temperature heat exchangers and apt external combustors, which should allow the system to operate at the actual micro gas turbine inlet temperature (900-950 °C).

This paper presents the plant layout and the control system employed for regulating the microturbine power and rotational speed. The experimental results obtained by the pilot plant in early 2004 are shown: the feasibility of such a plant configuration has been demonstrated, and the control system has successfully regulated the shaft speed in all the tests performed.

Finally, the plant model in TRANSEO, which was formerly used to design the control system, is shown to accurately simulate the plant behavior both at steady-state and transient conditions.

## INTRODUCTION

Externally-fired cycles have been studied in the past because they represent a valid option for the exploitation of "dirty" fuels, such as coal and biomass, without the complexity of a gasification section for fuel treatment [1]-[15]. The main drawback to such a configuration basically lies in the high temperature heat exchanger, which undoubtedly constitutes the most critical component of the whole plant, both for operation at high temperatures and the fouling problem on the exhausts side [10].

Previous studies have mainly focused on medium- and large-size plants for power generation: the present stress is on the development of economically feasible and technically reliable high-temperature heat exchangers to fit an externally-fired gas turbine. Despite reports of high-temperature heat exchangers working with exhausts from coal combustion at high temperatures, the state-of-the-art of ceramics for heat exchanger applications should still be considered at the research and development stage. The bayonet tube arrangement seems to be the most promising technique at the moment, even if hot gas leakages and heat dispersion from radiation are still inherent problems in the design of this component [10].

Although the poor technical and economic performance of externally-fired gas turbine cycles are still the major obstacles to their diffusion, the possibility of applying external combustion technology to the exploitation of renewable energy resources such as biomass has increased interest in small cycles which are capable of burning the available fuel "in situ": this should avoid additional transportation expenses and, thanks to possible cogenerative applications and integration with fuel pre-treatment without the complex and expensive technique of gasification, makes the plant more environmentally-friendly.

## NOMENCLATURE

| | |
|---|---|
| A | cross sectional area [$m^2$] |
| beta | pressure ratio |
| C | Compressor |
| cc | combustion chamber |
| $c_p$ | specific heat at constant pressure [kJ/kgK] |
| $c_v$ | specific heat at constant volume [kJ/kgK] |
| E | Expander |
| ECC | External Combustor Chamber |
| FO | Fractional Opening |

| | |
|---|---|
| ICC | Internal Combustor Chamber |
| $\dot{m}$ | mass flow rate [kg/s] |
| N | rotational speed [rpm] |
| p | pressure |
| P | power |
| PID | Proportional Integral Derivative controller |
| $\dot{q}$ | specific heat rate [kW/m] |
| Rec | recuperator |
| T | temperature |
| TIT | Turbine Inlet Temperature |
| TOT | Turbine Outlet Temperature [K] |

*Subscripts*

| | |
|---|---|
| nom | nominal |

*Greek letters*

| | |
|---|---|
| ρ | density [kg/m$^3$] |

## PREVIOUS RESEARCH ACTIVITIES

The collaboration between the Thermochemical Power Group and Ansaldo Ricerche (ARI), Genova, has led to the development of an externally-fired microturbine test rig, which has been successfully installed and operated at the ARI lab.

Initially, a major design effort was made to assess theoretically the performance of the test rig, based on a TA-80R Elliott microturbine (80kW at 28% efficiency, [16]), and a TRANSEO [17][18] simulation model for the off-design and transient analyses was developed and the results presented in [19][20]. Now, several tests have been carried out successfully on the test rig, and the measurements and experimental validation of the model are described here.

It should be noted that the test rig was mainly intended to assess the time-dependent behavior and control of the system, rather then demonstrating its potential performance: in fact, the emphasis given to the control assessment led to the installation of a metallic high-temperature heat exchanger, which limited the temperature downstream from the external combustor to values not higher than 800°C. In turn, this implied a poor thermodynamic performance for the plant, which, nevertheless, presented similar inertia (=> dynamic and transient behavior) to an actual externally-fired system.

The main limitations and problems of this cycle are basically linked to the high-temperature heat exchanger: thermal stresses must be reduced as much as possible, especially during the start-up procedure and the heating of the system. The relevant thermal inertia, coupled with the very short time response of the microturbine shaft, has to be properly considered in the development of the control system. Fouling could also be a problem for practical applications, but the use of natural gas during this experimental activity saved the ducts from that.

A real issue for the externally-fired cycles is represented by compressor surge: surge and sudden pressure oscillations can cause serious damage to the heat exchanger section, which is also the most expensive part of the plant. Previous studies [19] showed the risk of surge to be very low because of the low TIT of the EFmGT test rig: in fact, surge did not occur during the experiment.

## PLANT LAYOUT

The Externally Fired micro Gas Turbine (EFmGT) cycle is similar to a recuperated cycle where the combustion chamber is moved downstream from the expander, burning fuel at nearly atmospheric pressure. Since the basic idea was to integrate an existing recuperated microturbine in the EFmGT cycle, an additional heat exchanger had to be placed after the external combustion chamber, in order to heat the compressed air to the required TIT (Figure 1 illustrates the scheme of the plant, which was installed at the ARI laboratories). In this way the heat transfer is carried out by two distinct heat exchangers which are very different in terms of design specifications: the first one, Rec I, is a high-temperature metallic-type heat exchanger of large dimensions and high cost, while the second one, Rec II, is the commercial recuperator provided with the microturbine package.

The original combustor, which equips the microturbine, was retained in the final layout, even if not reported in Figure 1. It was used during start-up and for providing an additional increase in temperature to the TIT, when necessary.

The external combustor was already available in the laboratory: it is an atmospheric ceramic-insulated combustor for gas turbine hot gas path component testing. The gases coming from the expander are split into two streams (not reported in Figure 1): one goes through the combustor while the other is mixed with the exhausts at the combustor outlet. Additional combustion air ("comb air") needs to be provided: unfortunately, such a requirement unbalances the mass flows through the recuperators and increases the counter-pressure at the expander outlet. This last effect proved to be a major constraint during the experiment because it limited the external combustor outlet temperature to values below 700°C: in fact, for higher values, the expander outlet pressure exceeded the design constraint of about 900mmH2O relative pressure. In turn, as described later in the paper, only partial externally-fired configurations could be tested, where the internal combustor operated at a fixed heat rate.

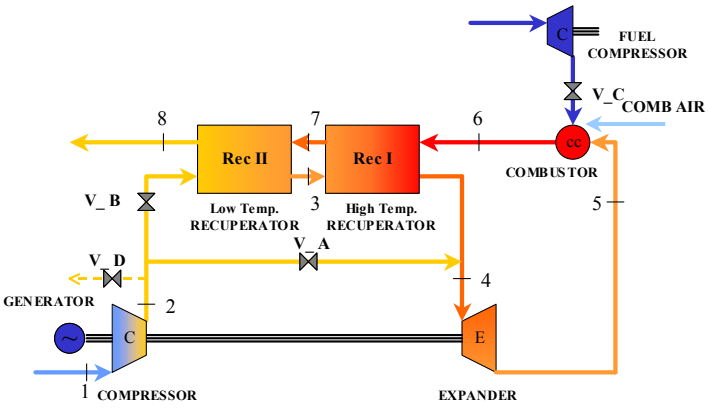


**Figure 1 - Schematics of the externally-fired microturbine cycle (EFmGT) with the main valves for cycle control**

In order to allow metallic super-alloys to be employed for Rec I, the T6 cannot exceed 800°C and, as a consequence, the TIT had to remain under 750°C during the experiment. However, the extendibility of the experimental plant is ensured by its modular scheme, where, in the future, the Rec I can be replaced with a ceramic one for testing the EFmGT at higher TITs. If the present TIT limit of 950°C is overcome, the microturbine should also be substituted by a cooled machine.

In the sketch of Figure 1 four valves are outlined:

- V_A for the air bypass of the recuperators,

- V_B for maintaining a constant pressure drop across V_A,
- V_C for the fuel to the external combustor,
- V_D as an emergency valve for the compressor.

Such a control scheme allows the control system to be de-coupled between a fast-response control loop, which is based on V_A and V_B, and has to prevent the microturbine rotor from reaching an excessive speed, and a slow-response control loop constituted by V_C, which should maintain V_A at its nominal position (normally open at reduced fractional opening, to allow a power step increase or decrease to be controlled) and optimize cycle performance. The purpose of each valve is the following:

- V_A must control the spool rotational speed, keeping it constant at the target value: this makes it a fairly critical device because of the low shaft mechanical inertia. As a result, V_A needs to be a fast-response valve and it directly acts on the TIT, since it allows part of the cold compressed air to mix with the hot compressed air coming from the recuperator section.
- V_B has to keep a constant pressure drop through V_A: in this way, it collaborates with V_A for the system control.
- V_C only needs to be tuned to the heat exchanger thermal inertia, which provides the largest delay of the whole system. For this reason, it can be a slow-response valve.
- V_D is a safety valve, normally closed.

Pictures of the actual test rig are presented in Figure 2 and Figure 3.

**Figure 2 - Front view of the microturbine recuperator (bottom left of the picture), which has been displaced from its original position within the package (courtesy of ARI)**

The actual plant has to comply with four major constraints under all operating conditions: the temperature at the external combustor outlet (T6) must not exceed 800°C, the temperature at the exhaust inlet of the recuperator (T7) must not be higher than 650°C, the compressor surge margin must always be enough to ensure the dynamic stability of the plant, the machine spool speed must be kept below an overspeed of about 10% of the nominal speed (68000rpm).

The power produced by the plant is dissipated by a resistence bank. In this way, the electrical efficiency of the generator and the power electronics can be estimated from the calculation of the thermodynamic power available at the shaft. Such an efficiency proved to be very significant, as expected, due to the relatively poor performance of the electrical conversion system (see Figure 14).

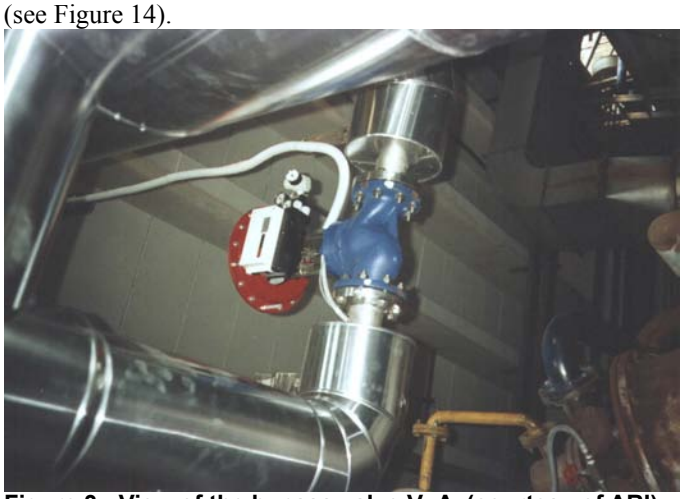

**Figure 3 - View of the bypass valve V_A (courtesy of ARI)**

## TRANSEO MODEL

The plant layout was modeled in TRANSEO: the sketch of the model layout is reported in Figure 4. Such a model represents the latest development of the one presented in [20], which was used for preliminarily assessing the off-design and transient performance of the plant. Now, thanks to the availability of the first experimental results, the model has been upgraded and the results validated.

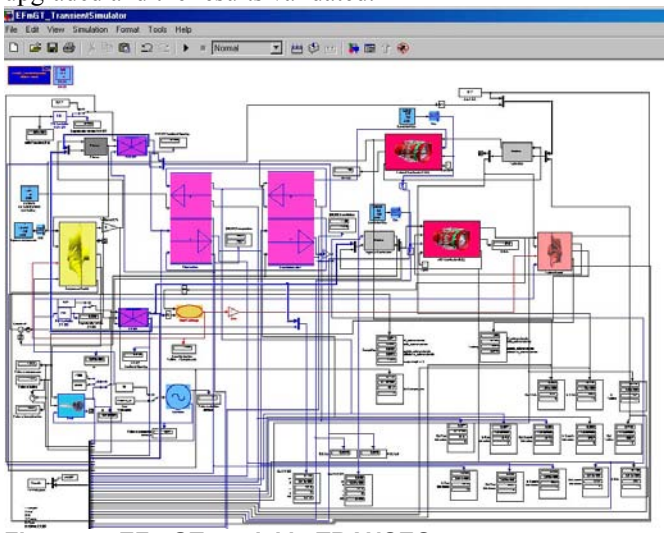

**Figure 4 - EFmGT model in TRANSEO**

It is worth summarizing here the main features of the EFmGT simulator tool. Turbomachinery was represented with characteristic curves provided by ARI; then, the heat exchange between the compressor and the expander had to be included in order to obtain the true compressor outlet temperature; the heat storage within the rotating parts was also considered [17]. Generator efficiency was found as a result of the validation process, and the electrical efficiency variation at part-load was incorporated in the "Generator" block with a third order polynomial (see Figure 14). The internal and external combustion chambers (ICC and ECC, respectively) were simulated with the same model, adapted to the different features of these two devices. The key-components of the EFmGT, which are the two recuperators, were modeled

according to the approach outlined in [19] and fully described in [18]: each recuperator has been represented by on e heat exchanger model. The finite difference mathematical model (Figure 5) assumes that convective transport dominates the diffusion between adjoining fluid elements and that the mass storage within each control volume is negligible in comparison to the thermal storage in the fluid and metallic cells: as a consequence, the temperature change becomes the main phenomenon which dominates the transient behavior of the heat exchanger. In general, the partial difference energy equation can be written as follows:

$$\rho_{j,i} c_{v_j} A_j \frac{\partial T_{j,i}}{\partial t} = - c_{p_j} \dot{m}_j \frac{\partial T_{j,i}}{\partial x} + \dot{q}_{j,i} \qquad (1)$$

where j=h (hot), m (matrix), c (cold), v (vessel).

The heat source terms depend on the part under consideration (h,m,c,v) and they take into account the convective heat transfer between the fluids and the transfer surfaces, the heat dispersion to the environment at $T_{amb}$, and the longitudinal conductivity of the matrix and the vessel. Equation (1) is integrated with time according to an implicit scheme that allows all the new, unknown temperatures to be arranged in a linear system whose solution provides the new temperatures of the next time step.

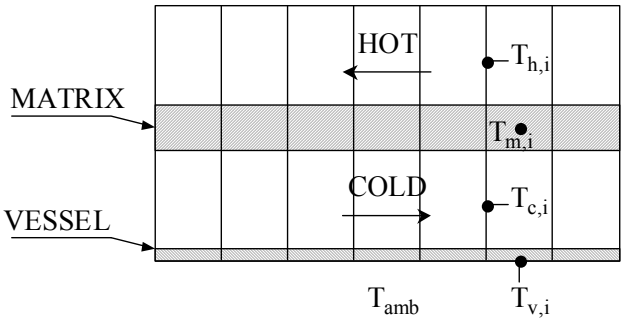


**Figure 5 - Discretization mesh of the heat exchanger model**

| | |
|---|---|
| **Compressor** | |
| Internal metal mass exchanging heat with air | 30 kg |
| Available internal heat exchanging surface | 0.344 m2 |
| **Turbine** | |
| Internal metal mass exchanging heat with air | 40 kg |
| Available internal heat exchanging surface | 0.34 m2 |
| **Rotating shaft** | |
| Rotational inertia | 0.0243 kg·m$^2$ |
| **Recuperator (Rec II)** | |
| Internal metal matrix (plates and fins) | 120 kg |
| External metal inertia (vessel) | 3 kg |
| **High temperature heat exchanger (Rec I)** | |
| Internal metal matrix (plates) | 1500 kg |
| External metal inertia (vessel) | 150 kg |
| **External combustion chamber (ECC)** | |
| Ceramic mass | 50 kg |
| **Piping** | |
| Total volume on compressed air side | 0.3 m3 |

**Table 1 - Main assumptions for transient calculations**

The main assumptions for cycle component behavior under unsteady conditions are reported in Table 1. Valve delays proved to be negligible because they were in the order of 0.1s (V_A and V_B are pneumatically actuated valves).

## STEADY-STATE RESULTS

The initial experimental matrix of plant layout in Figure 1 was organized into four main phases.

First, stationary tests of the plant in a "conventional" internal combustion configuration: in these tests the external combustion chamber was turned off while the heat was solely provided by the microturbine combustor; the microturbine was operated in an "enhanced" recuperated cycle, because of the presence of Rec I, which was crossed by the air and exhaust flows.

Second, stationary tests of the plant in a partial external combustion configuration: in these tests the exhausts from the turbine were sent to the external combustor, which increased their temperature and sent them to the Rec I inlet. The internal combustion chamber was kept at a low heat rate.

Third, control tests of the plant in partial external combustion configuration (as in the second phase) by regulating the shaft speed with the original microturbine control system, by acting on the ICC fuel valve.

Fourth, control tests of the plant in complete external combustion configuration: in these tests the ICC was turned off and all the heat provided by ECC.

The experimental matrix was completed successfully, except for the last phase, where the excessive counter-pressure at the turbine outlet prevented the tests from increasing the ECC outlet temperature above about 700°C: this required the ICC to be on, even if at a minimal heat rate, during all the tests. This limit will be overcome by designing a new external combustor for the plant, which, instead, used an existing one upgraded for the EFmGT application.

The results obtained during the first phase of tests, for electrical power ranging from 50kW to 15kW, are reported from Figure 6 to Figure 17. In such diagrams the simulated data, recorded at steady-state conditions, are compared against the measurements, showing good agreement.

Three points need to be discussed in more detail: the behavior of the compressor outlet temperature, the obtained curves for electrical-mechanical efficiency and the measured air flow.

The compressor outlet temperature, reported in Figure 6, shows a sort of discontinuity at the last point recorded, at the lowest power: since such a measurement has been verified repeatedly, experimental error can be excluded. The delivery pressure (Figure 10) continually decreases from high power to low power levels, hence it is likely that the temperature increase measured at the compressor outlet is due rather to an anomalous behavior of the heat exchange with the turbine (in the order of 20kW of thermal power) than to a sudden drop in compressor efficiency.

With regard to the power and electrical-mechanical efficiency (Figure 13 and Figure 14), the measurements only provided the electrical power record, without any information on the thermodynamic power available at the shaft. Hence, in this case, the simulation was used to calculate such a theoretical thermodynamic power; then, after assuming the mechanical loss in the bearings (constantly equal to 2kW, because of the constant rotational speed), the electrical loss in the turbogenerator and the power electronics could be inferred

(Figure 13): as expected, the electrical loss was dominated by power electronics dissipation, which is roughly constant all over the power range considered. Figure 14 reports the non-dimensional efficiencies (only electrical and mechanical-electrical together): the resulting interpolating curves are very similar to a standard curve for microturbine off-design conditions [21].

Finally, the slight difference between the compressor map and the measured flow, in Figure 15, is due to small leakages in the plant, in the order of 2% of the intake air flow.

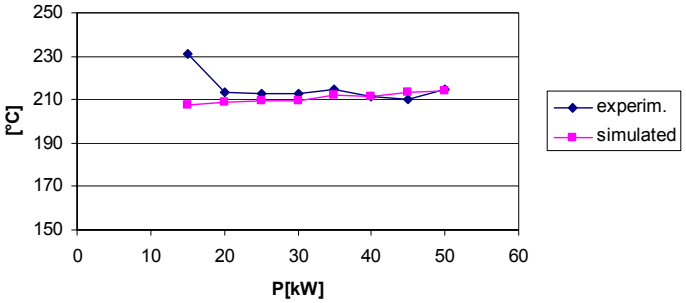


**Figure 6 - Compressor outlet temperature, T2**

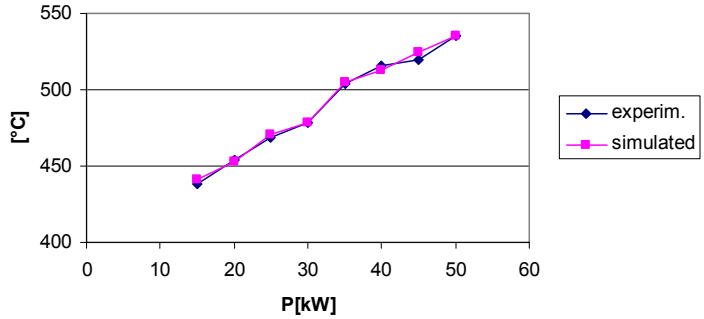


**Figure 7 - Rec I air outlet temperature, T4 (equal to T4 because the bypass valve is closed)**

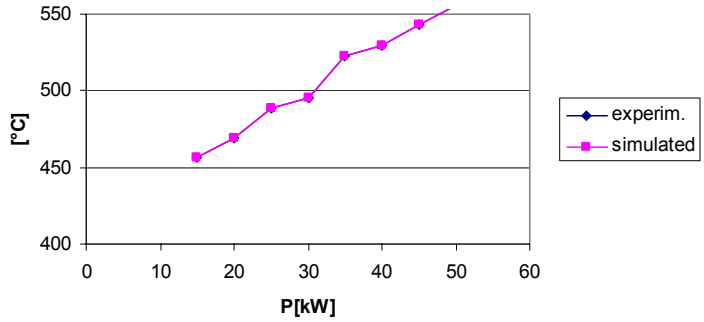


**Figure 8 - Turbine outlet temperature, T5**

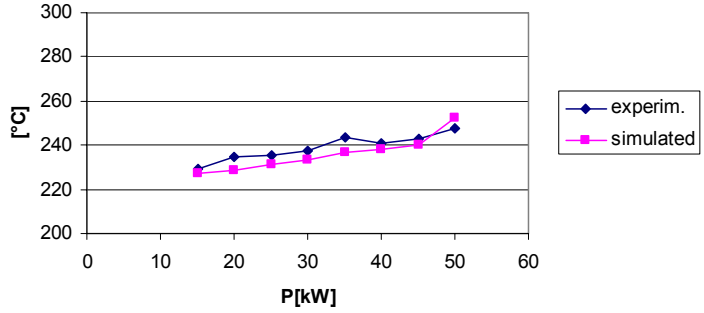


**Figure 9 - Rec II exhaust outlet temperature, T8**

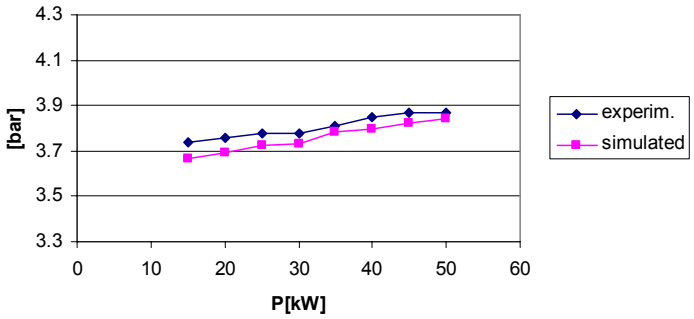


**Figure 10 - Compressor outlet pressure, p2**

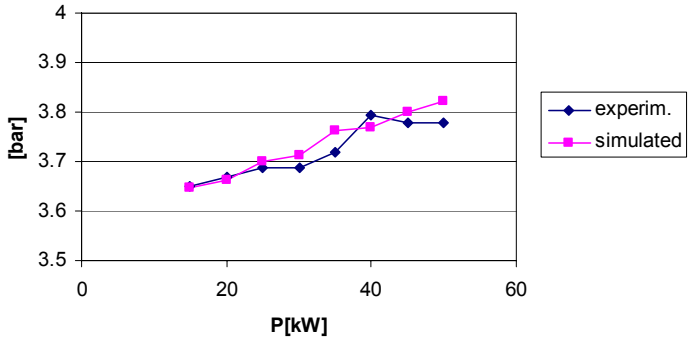


**Figure 11 - Rec I air outlet pressure, p4**

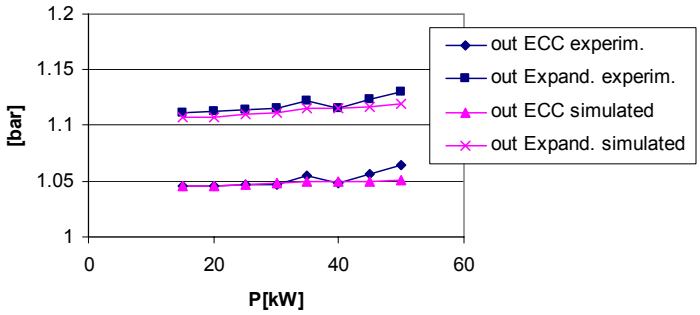


**Figure 12 - Pressures at ECC outlet and expander outlet**

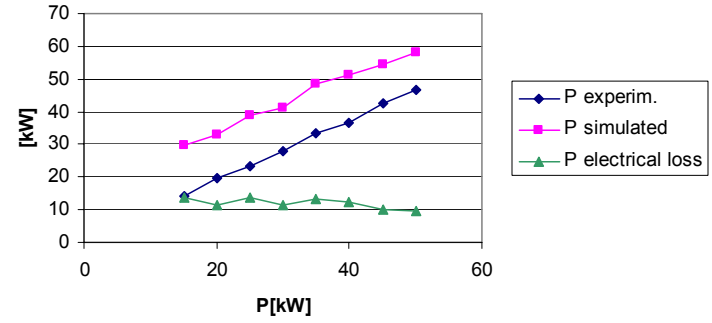


**Figure 13 - Power measured, power theoretically available at the shaft (simulated), electrical power loss**

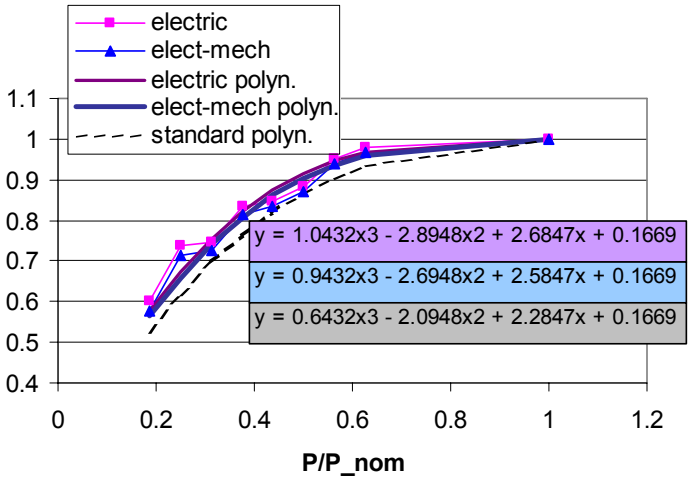


**Figure 14 - Non-dimensional efficiencies, electrical efficiency and electrical-mechanical efficiency (nominal values are 0.85 and 0.975 for the electrical and mechanical efficiencies, respectively)**

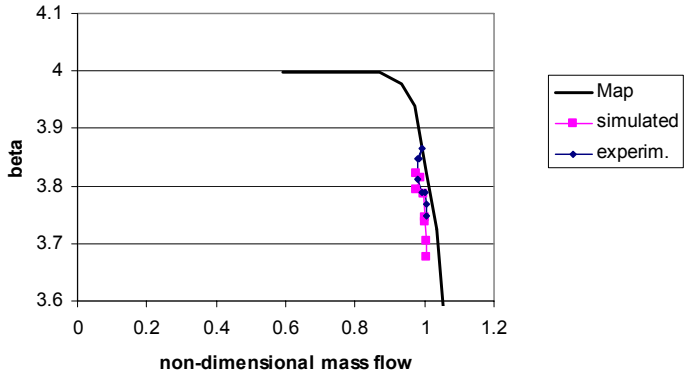


**Figure 15 - Compressor operating points**

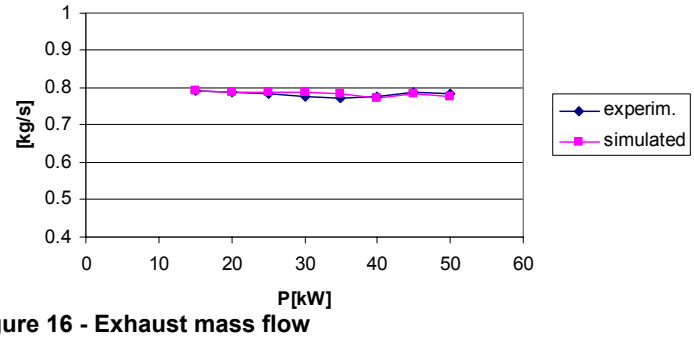


**Figure 16 - Exhaust mass flow**

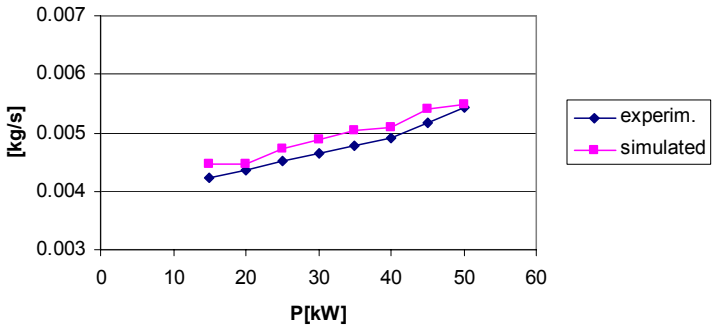


**Figure 17 - Natural gas mass flow to internal combustor**

## TRANSIENT RESULTS

The transient measurements illustrated here refer to the fourth phase of the scheduled experimental matrix. As already stated, differently from the original plans, in these tests the internal combustion chamber was on at a constant heat rate of about 80-150kW, depending on the test to be performed. The results for a load disturbance of 5kW are reported from Figure 18 to Figure 23 (starting from about 26kW electrical power, power step decrease of 5kW, then, after 300s, power step increase back to the initial power; see Figure 18): the "Reference" experimental curve is compared to the simulated one. Albeit only this case is reported, several other tests experimentally demonstrated the feasibility of the control strategy: the goal of the project has been achieved.

With regard to the EFmGT model, the aforementioned diagrams show a good representation of the transient behavior of the entire system, so that, now, the model can be independently used for further improving the control system as well as theoretically assessing alternative control strategies. Some differences between measurements and predictions occur in the small oscillations of the rotational speed N when the original power is restored: they are basically due to the bypass valve characteristic curve and local gain, which is higher in the model than in the real system.

The simulated ICC inlet temperature (Figure 20) shows higher peaks corresponding to the power steps: apart from the thermal inertia of the piping, not included in the model, the mismatch could also be due to the thermocouple shield delay, which was not included in the model.

The measured trace of counter-pressure valve (V_B) fractional opening (Figure 22) shows quite a disturbed behavior, which was due to the fluidodynamic disturbances in the differential pressure probe (the controlled variable). In this respect, the design gain of the PID controller had to be reduced by a factor 0.2 in order to obtain a stable valve behavior: it follows that the margins for improvement are high on this side.

Finally, Figure 23 shows the transient heat storage in the turbomachinery (obtained from calculation), which is obviously much higher for the expander than for the compressor. The effect of this real phenomenon is described in the next paragraph.

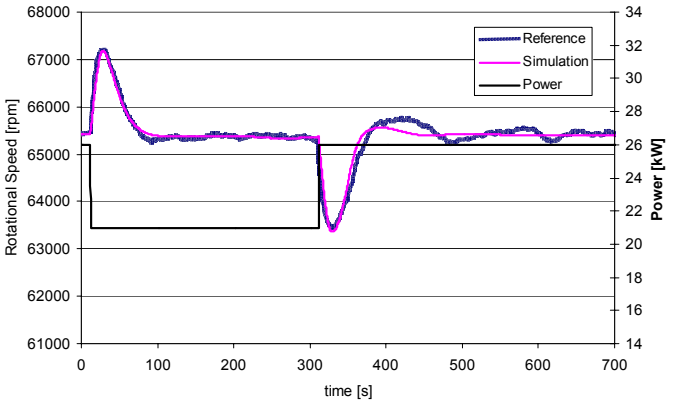


**Figure 18 - Shaft speed response to load step variations**

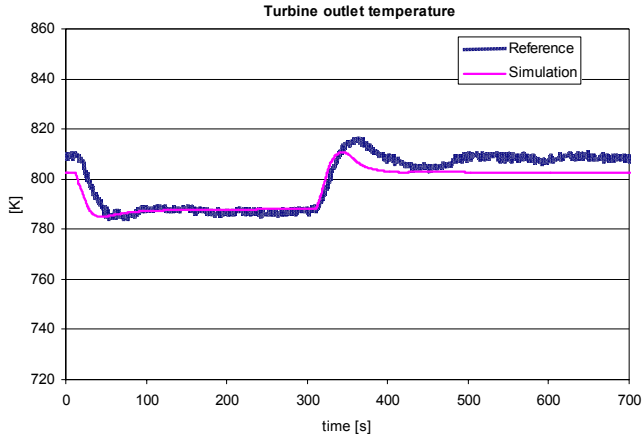


**Figure 19 - Turbine outlet temperature, T5**

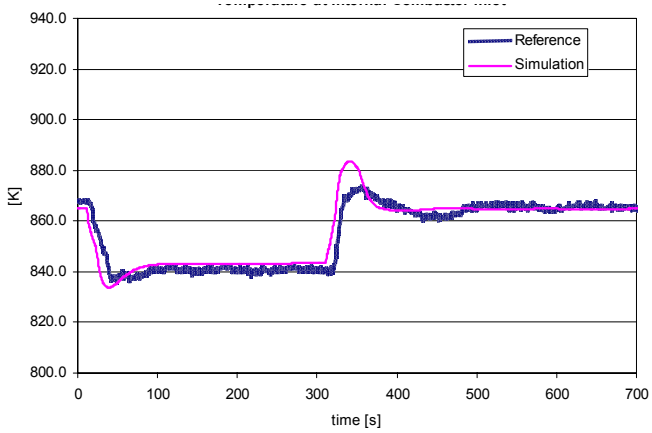


**Figure 20 - Temperature at internal combustor inlet**

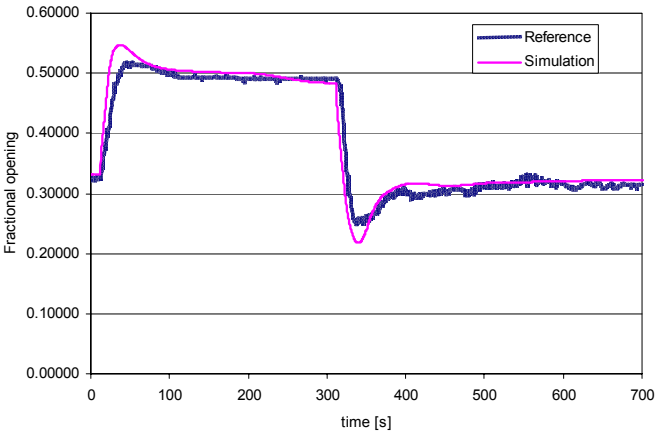


**Figure 21 - Fractional opening of the bypass valve**

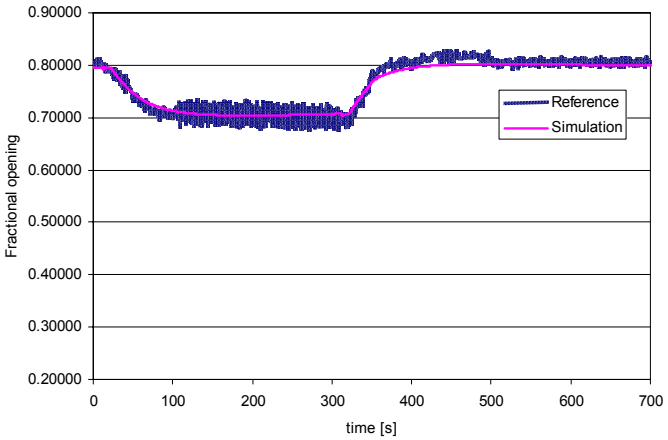


**Figure 22 - Fractional opening of the counter-pressure valve**

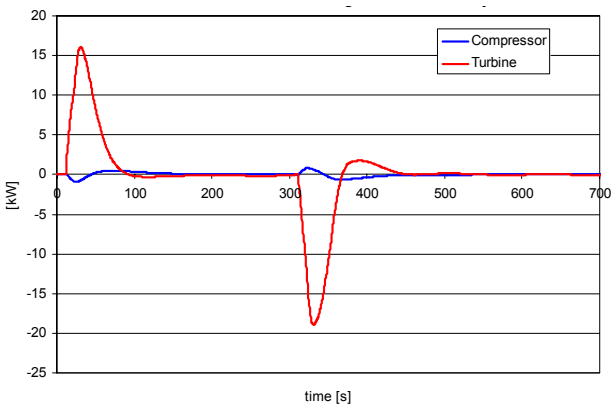


**Figure 23 - Heat storage in the turbomachinery (heat exchanged between the fluid and the rotating parts; heat is positive when received by the fluid)**

## SENSITIVITY ANALYSIS

Once the EFmGT model was validated, it was used for performing sensitivity analyses to understand better the behavior and the operational limitations of the plant. The simulation showed previously is used as a reference (violet line) in the following simulations.

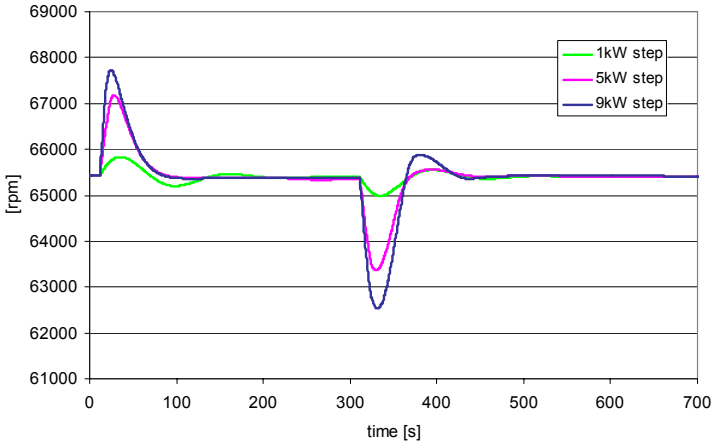


**Figure 24 - Rotational speed behavior at three different load steps**

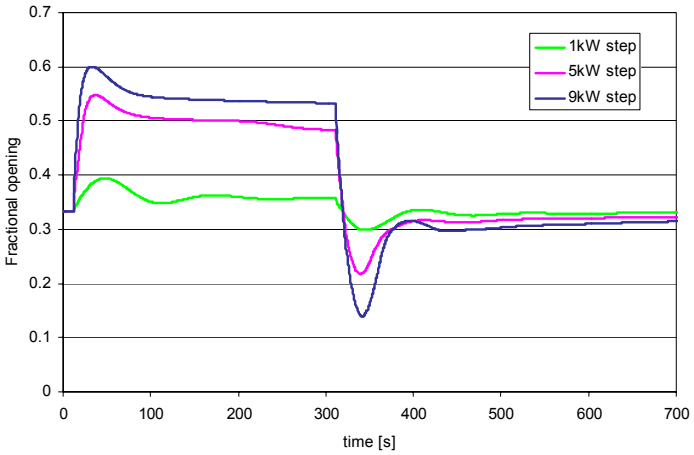


**Figure 25 - Fractional opening behavior of the bypass valve at three different load steps**

The first simulation was done to assess the plant behavior at different load steps: ±1kW and ±9kW were compared to the reference ±5kW. The results are very good (Figure 24 and Figure 25), since the plant is able to keep the rotational speed under control without instabilities or overspeed. Only the smallest power step shows some oscillations in rotational speed, mainly due to the local gain of the bypass valve.

The second simulation aimed at assessing the importance of the counter-pressure valve (V_B) in helping the bypass valve (V_A) to control N. In this case, the correction factor applied to the V_B controller gain (0.2) was first increased to 0.5 (full control) and then set to 0 (no control). It was impossible to use a factor equal to 1 because instabilities occurred. The results (Figure 26) show how little influence V_B has on the rotational speed behavior. For this reason, it is possible that the control system could be simplified by removing the V_B valve while retaining almost the same performance. Nevertheless, experimental tests will be required to further investigate this option.

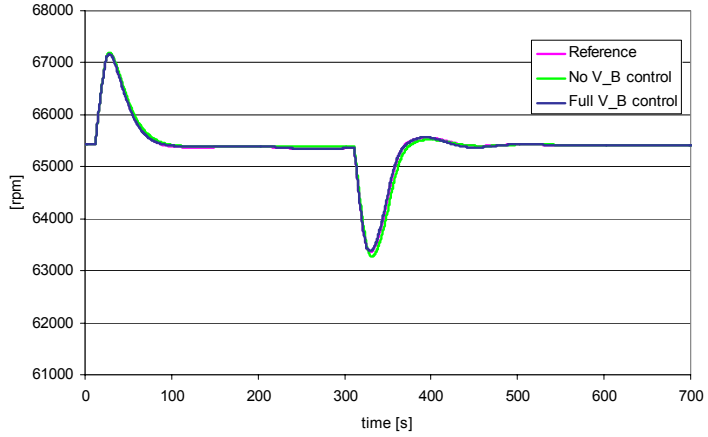


**Figure 26 - Rotational speed behavior varying the V_B control**

The third and last simulation focused on plant performance varying two cycle conditions: the influence of the thermal storage in the turbomachinery was firstly investigated by neglecting this effect and comparing the new transient behavior to the reference one; then, to study a configuration similar to a high-temperature hybrid fuel cell system [23], a volume of $10m^3$ was considered as positioned between the compressor and the recuperator inlet.

Figure 27 and Figure 28 show that the thermal inertia of the turbomachinery mainly affects the turbine outlet temperature behavior [22], while the rotational speed seems to be only marginally influenced: these results are in accordance with [17].

The increase in volume on the compressed air side has major effects on all the system parameters since it smoothes out rapid shaft responses and introduces a significant delay in the time-response of the system, which is evident from the oscillatory behavior of N. In this case, surge may occur at a load step increase, because N decreases while pressure is retained almost constant by the volume: this problem did not appear in the simulations because of the large surge margin of the starting point (more than 30%), but it should be carefully monitored.

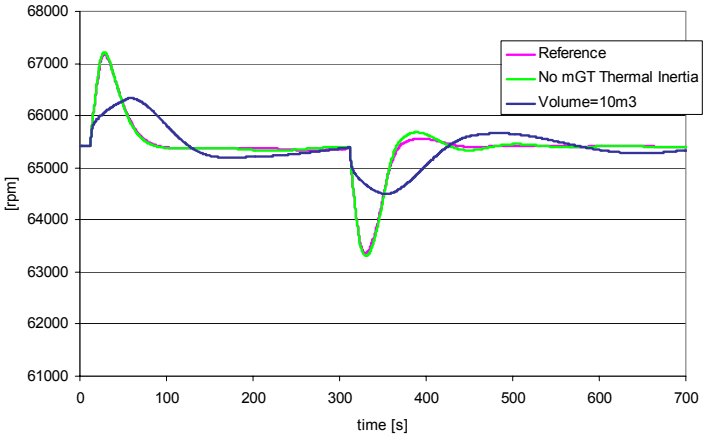


**Figure 27 - Rotational speed behavior varying cycle conditions**

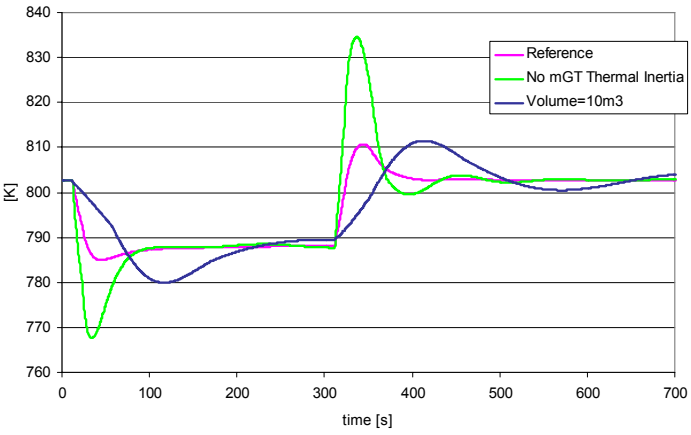


**Figure 28 - TOT behavior varying cycle conditions**

## CONCLUSIONS

This paper presents the experimental results and model validation of the world's first Externally Fired micro Gas Turbine plant. The test facility was designed and built at ANSALDO Ricerche gas turbine test rig, in collaboration with the TPG, for testing the feasibility of a control strategy for externally fired gas turbines at a laboratory scale.

The experiment successfully demonstrated the controllability of the cycle, even employing an 80kW commercial microturbine, which has a significantly more "nervous" shaft response than a large gas turbine.

Several tests were performed to assess the off-design behavior of the cycle and then the dynamic behavior. Further improvements in cycle layout and component design will enhance the control of the system at part-loads and will extend the operational range of the test rig.

The TRANSEO code was employed for modeling and simulating the EFmGT cycle at off-design and transient conditions. The EFmGT model was validated against experimental measurements, and showed good agreement. The validated model was finally employed for assessing the system behavior under different conditions, such as higher load steps and large volumes on the compressed air side.

The results and operational experience gained during the project are expected to provide a good basis for both improving the existing test rig and extending its application to other cycles, such as high-temperature hybrid fuel cell systems.

## ACKNOWLEDGMENTS

The authors wish to thank F. Rosatelli and C. Mao of ARI for their support during the study and analysis of the EFmGT cycle.

## REFERENCES

[1] C. L. Vandervort, M. R. Bary, L. E. Stodard, S. T. Higgins, 1993, "Externally Fired Combined Cycle Repowering of Existing Steam Plants", ASME paper 92-GT-359.

[2] F. Farina, P. G. Avanzini, "Problems Related to the Design of an IFGT Test Facility", 1993, ASME COGEN TURBO, Vol. 8.

[3] G. Crosa, L. Fantini, G. Ferrari, L. Pizzimenti, A. Trucco, "Steady State and Dynamic Behavior of an Indirect Fired Gas Turbine Plant", 1998, ASME paper 98-GT-167.

[4] S. B. Ferreira, P. Pilidis, "Comparison of Externally Fired and Internal Combustion Gas Turbines Using Biomass Fuel", 2001, Journal of Energy Resources Technology, 123, pp.291-296.

[5] J. Yan, "Externally Fired Gas Turbines, The State-of-the-Art of Research and Engineering Development", 1998, Technical Report, Royal Institute of Technology, Sweden, ISSN 1104 – 3466.

[6] T. O'Doherty, A. J. Jolly, C. J. Bates, 2001, "Analysis of a bayonet tube heat exchanger", Applied Thermal Engineering, 21, pp.1-18.

[7] P. G. Lahaye, E. R. Zabolotny, 1989, "Externally Fired Combined Cycle (EFCC), ASME-COGEN-TURBO meeting, Nice, France, pp263-274.

[8] S. Consonni, E. Macchi, F. Farina, 1996," Externally Fired Combined Cycle (EFCC). Part A: Thermodynamics and Technological issues", ASME paper 96-GT-92

[9] S. Consonni, E. Macchi, F. Farina, 1996, "Externally Fired Combined Cycle (EFCC). Part B: Alternative Configurations and Cost Projections", ASME paper 96-GT-93

[10] L. Tumolo, "Bayonet Heat Exchanger Complete Model for Externally Fired Turbine Cycles", 2002, Master Thesis, TPG-DiMSET, Università di Genova, Genova, Italy (in Italian).

[11] P. R. Solomon, M. A. Serio, J. E. Cosgrove, D. S. Pines, Y. Zhao, R. C. Buggeln, S. J. Shamroth, "A Coal-Fired Heat Exchanger for an Externally Fired Gas Turbine", 1996, Journal of Engineering for Gas Turbines and Power, 118, pp.23-31.

[12] D. Marroyen, S. Bram, J. De Ruyck, "Progress of an Externally Fired Evaporative Gas Turbine Cycle for Small Scale Biomass Gasification", 1999, ASME Paper 99-GT-322.

[13] B. Elmeegard, B. Qvale, "Analysis of Indirectly Fired Gas Turbine for Wet Biomass Fuels Based on Commercial Micro Gas Turbine Data", 2002, ASME paper GT-2002-30016.

[14] S. B. Ferreira, 2002, "Thermoeconomic Analysis and Optimisation of Biomass Fuel Gas Turbines", Ph.D. Thesis, Cranfield University.

[15] D. Chiaramonti, G. Riccio, F. Martelli, 2004, "Preliminary design and economic analysis of a biomass fed micro-gas turbine plant for decentralised energy generation in Tuscany", ASME Paper, 53546

[16] TA-80R, data from commercial brochure, Elliott Energy Systems.

[17] A. Traverso, "TRANSEO Code For The Dynamic Simulation Of Micro Gas Turbine Cycles", 2005, ASME Paper 2005-GT-68101.

[18] A. Traverso," TRANSEO: A New Simulation Tool For Transient Analysis Of Innovative Energy Systems", 2004, Ph.D. Thesis, DiMSET, Università di Genova, Genova, Italy.

[19] A. Traverso, L. Magistri, R. Scarpellini, A.F. Massardo, "Demonstration Plant and Expected Performance of An Externally Fired Micro Gas Turbine for Distributed Power Generation", 2003, ASME Paper 2003-GT-38268.

[20] A. Traverso, F. Calzolari, A.F. Massardo, "Transient Analysis of and Control System for Advanced cycles based on Micro Gas Turbine Technology", 2003, ASME Paper 2003-GT-38269 (accepted for Transactions).

[21] L. Magistri, "Hybrid Systems for Distributed Generation", 2003, Ph.D. Thesis, DiMSET, Università di Genova, Genova, Italy.

[22] P. Pilidis, N. R. L. Maccallum, "The Effects of Heat Transfer on Gas Turbine Transients", 1986, ASME paper 86-GT-275.

[23] M. Ferrari, A. Traverso, A. F. Massardo, "Control System For Solid Oxide Fuel Cell Hybrid Systems", 2005, ASME Paper 2005-GT-68102.